International Journal of Science and Research (IJSR)
ISSN (Online): 2319-7064
Index Copernicus Value (2013): 6.14 | Impact Factor (2013): 4.438

A Facile Replicable Route To Graphene Production Using Anionic Surfactant

Udensi, S. C.[1], Ekpunobi[2] A. J., Ekwo, P. I.[3]

[1]Department of Physics, Federal University of Technology Owerri, P.M.B. 1526 Owerri, Imo State, Nigeria
and Department of Physics and Industrial Physics, Nnamdi Azikiwe University, Awka, Nigeria

[2, 3]Department of Physics and Industrial Physics, Nnamdi Azikiwe University, Awka, Nigeria

Abstract: ***Graphene monolayer and multilayers have been prepared through functionalization of the graphite powder with anionic surfactant to make the hydrophobic graphite more hydrophilic and sheared using different agitator blades. EDX revealed high weight percent yield and non production of graphene oxide which usually affect the conductivity of graphene. Raman microscopy confirmed that band peaks are functions of graphene multilayer. The plot of intensity band ratios of D:G versus reciprocal of lateral flake size validated a D:G band ratio of 0.48 for our starting powder, confirmed a slope of 0.17 as obtained using other sources of graphite powder elsewhere, and demonstrated the production of mean lateral flake sizes of 1, 2, 3, and 9 layers of graphene. Also, the I_D/I_G versus I_D'/I_G plot of the graphenes showed a slope of 2.21 as against those reported for defected graphenes, attesting to the production of defect-free graphene monolayer and multilayer.***

Keywords: Graphene, Functionalization, Turbulence, defect-free, Raman microscope.

1. Introduction

Graphene is a two dimensional monolayer of carbon atoms tightly packed in a honeycomb-like lattice, which is the fundamental building block of graphitic materials of several other dimensions [1]. It a zero band gap, high carrier mobility and concentration material, with a nearly ballistic transport property at room temperature [2]. Researchers are united in their quest to a cost effective route to graphene production, because of their intriguing electrical, mechanical [3], thermal [4] etc. properties. This is promising owing to its anticipated range of technological applications, which include but are not limited to optoelectronics, foldable devices, conductive inks, fire retardants, composites [5].

Expectedly, these researchers have reported several processing routes to graphene production, among which are oxidation of graphite powders [6], catalytic unzipping of carbon nanotubes [7], thermal shock exfoliation [8], etc. - with all these routes having varied sub routes. Most of these methods require functionalization of graphite powder (GP) with chemicals which introduce 'defects' sites to graphene, therefore hampering and, most times, extinguishing their electronic properties [9].

Furthermore, the surface free energy of graphene is 46.7 mJ/m^2 compared to 54.8 mJ/m^2 for graphite flake (GF) at room temperature and 62.1 mJ/m^2 for graphene oxide (GO). These energy differences account for the hydrophobic nature of graphene [10] and its difficulty in exfoliation in water irrespective of the shear force applied. Hence, in order to strike a balance between the total surface energy of GP [11] and that of the liquid in which graphene is to be exfoliated, a series of optimization techniques would be required to modify the hydrophobicity of graphene, make it more hydrophilic, without tampering on its physical properties.

Literatures have reported exfoliation of graphene from different harsh liquid solutions, which in turn introduced defects and damage the conductivity properties of graphene. In this paper, mild anionic surfactants would be used to functionalize the GNs in water before consigning the resulting aqueous mixture to localised turbulent high shear rates [12], using a household blender. The rotating blade has a Reynolds number (Re) [13] given by;

$$\mathrm{Re}_{Blade} = \frac{\rho N D^2}{\mu} \quad \text{..... (1)}$$

where ρ, μ, D and N are density (1000kg/m^3), viscosity (0.001 Pa s), diameter of the agitator and rotational speed respectively. Strong spatial and temporal variations [12, 14] were generated by the turbulent shear rate, $\dot{\ell}$, which in turn was controlled by the rate of energy dissipation, (per unit mass) [15].

$$\dot{\ell} = \sqrt{P/V\mu} \quad \text{..... (2)}$$

This study is important, if we desire to produce graphene with pristine physical and chemical properties, which would result in more efficient graphene-based devices. In this paper, reports on analytical investigation using raman spectroscopy are presented.

2. Experimental

2.1. Materials and Method

Graphite powder (SP-1 grade) containing 1 ppm silicon and trace amount of caesium, and zinc was obtained from Bay carbon. The anionic surfactant and hydrotropes used were contained in a household washing liquid (Morning fresh).

Graphite powder (GP) and anionic surfactant were mixed into a paste in a ratio of 4:1 and left for 12 hours. The paste

was then sheared for 60 minutes in a house- hold blender containing 250ml deionized water, using a two-, three and four blade agitator (with different turbulent shear rates), at 20 minute interval. Successively, 250ml of deionized water was added to the mixture until the total volume became 1500ml. After each addition, the resulting mixture was sheared for 20 minutes.

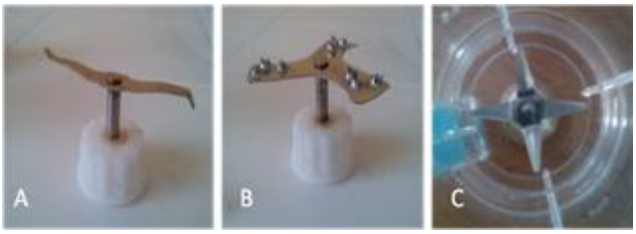

Figure 1: Images of (A) two blade (B) three blade and (C) four blade agitators used in shearing of the GP

Five samples (A-E) of supernatant were collected after 45 minute intervals, centrifuged for 30 minutes at 3000rpm, filtered, dried in the oven for 3 hrs, and analysed using Renishaw inVia raman microscope (wire 2.0 software) at 633nm excitation wavelength and, x20 objective lens.

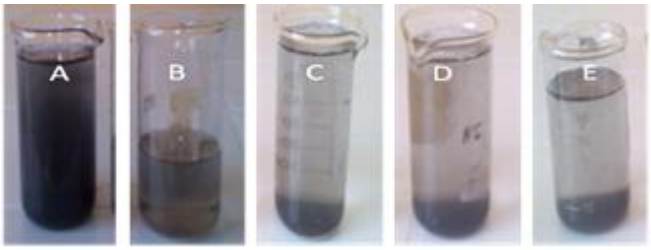

Figure 2: Size selection of graphene from the supernatants labelled as samples A – E

3. Results and Discussion

Raman characterization of graphene and graphene-based materials [16,17] is advantageous because of its outstanding, non-destructive nature, on sample materials. The raman spectra of the dried samples, taken under room temperature conditions are presented in figure 5 (Figure 5a shows the raman spectrum of GP, reference spectrum, while figures 5b to 5e show the spectra of samples A-D corresponding to 45, 90, 135, 180 minutes respectively. The D, G and 2D bands peaks are fingerprints of multilayer graphene [16,18]. Liquid phase exfoliation of graphene is fraught with by-product of graphene oxide, however, our EDX measurement revealed a high (84.49 wt %) yield of carbon for Sample C (figure 4). The remaining signals came from minuscule amount of impurities from the graphite powder, the anionic head (sulphates) of the surfactant, the hydrotropes, and other adsorbates on the graphene surfaces.

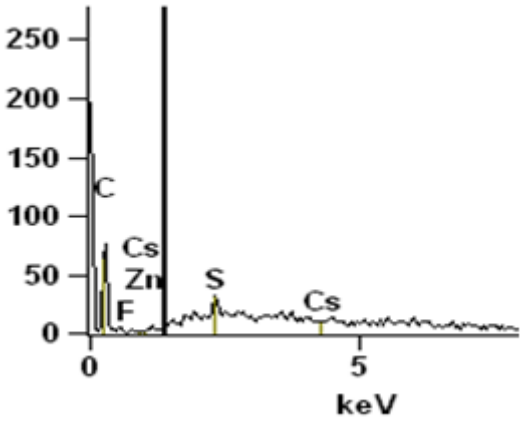

Figure 3: EDX showing high yield of graphene and the non-existence of GO.

Bulk and edge defects affect the symmetry conditions of energy versus wave vector characteristics of graphene, and encourage inter/intra valley processes between/within its D and D' bands [19, 20]. The extents of these defects have direct relationship to the ratios of the intensity peaks of the D bands to those of the G bands, the larger the defects the larger the ratio. Elsewhere, studies show that if graphene nanosheets contain only edge defects (an intrinsic property of nanosheets) [21,22], then the D:G intensity peak ratio would be connected approximately to the mean lateral flake size, $\langle L \rangle$ by

$$\frac{I_D}{I_G} \approx \left(\frac{I_D}{I_G}\right)_{GP} + \frac{k}{\langle L \rangle} \quad \text{..... (2)}$$

where $(I_D/I_G)_{GP}$ is the graphite powder D:G band ratio, and k, a constant approximately equal to 0.17 [23]. Presented in figure 4 is the I_D/I_G versus 1/< L > plot from our samples, the intercept is approximately 0.48, and confirmed from table 1. Also, if the lateral flake size of the crystallite were assumed large, then 1/< L > would approach zero, and the ratio of peak intenstites D to G becomes equal to our experimental intercept (i.e 0.48). This is a further pointer showing non-introduction of edge defects during graphene exfoliation.

Table 1: Raman peak ratios of GP and samples A, B, C, and D

	I_D/I_G	$I_{D'}/I_G$	$I_D/I_{D'}$	I_{2D}/I_D	I_{2D}/I_G
GP	0.48	0.49	0.98	1.19	0.58
A	0.50	0.47	1.001	1.24	0.62
B	0.53	0.48	1.086	1.18	0.62
C	0.57	0.49	1.136	1.10	0.56
D	0.62	0.50	1.266	1.33	0.82

Table 2: Sample mean lateral flake size and its reciprocal

	< L >	1/< L>
Sample A	8.5	0.12
Sample B	3.4	0.29
Sample C	1.88	0.53
Sample D	1.21	0.83

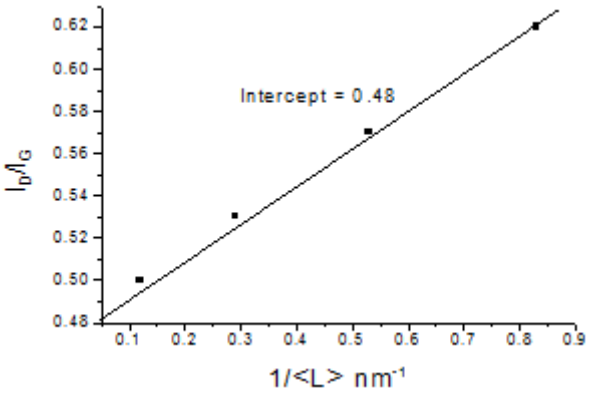

Figure 4: I_D/I_G versus reciprocal of lateral mean size

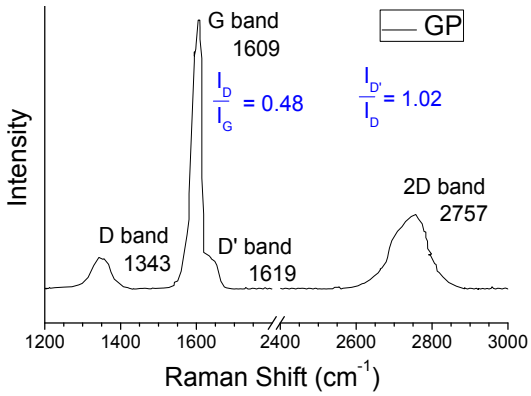

Figure 5a: Raman spectrum of pristine graphite (Bay carbon)

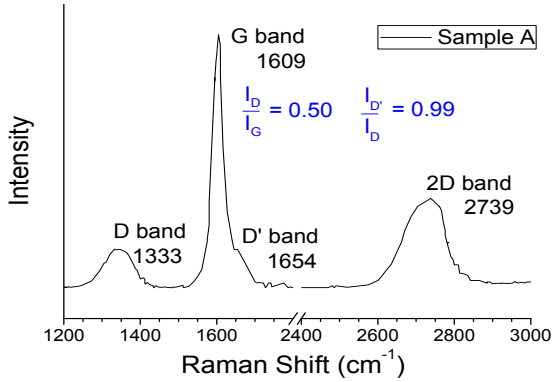

Figure 5b: Raman spectrum of graphene collected from supernatant after 45 mins

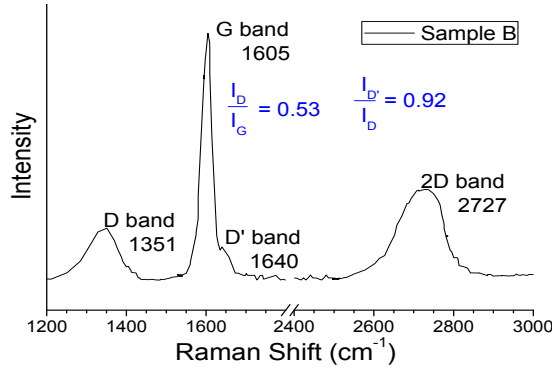

Figure 5c: Raman spectrum of graphene collected from supernatant after 90 mins

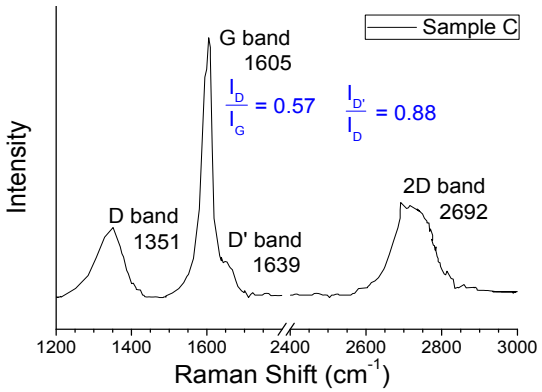

Figure 5d: Raman spectrum of graphene collected from supernatant after 135 mins

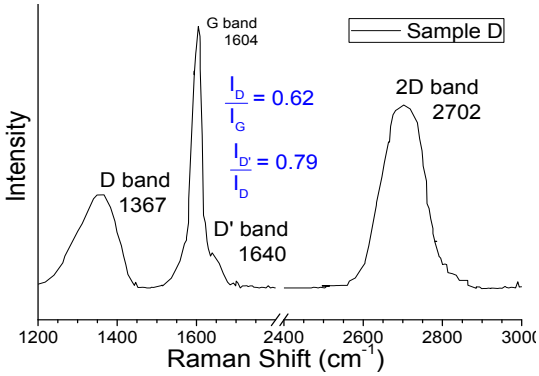

Figure 5e: Raman spectrum of graphene collected from supernatant after180 mins

The slope of our straight line graph is 0.17, in conformity to the results reported elsewhere [23], an indication that equation 2 is a good approximation for size selection of graphene sheets, that is,

$$L = \left(\frac{0.17}{I_D/I_G - 0.48} \right) \quad \text{..... (3)}$$

Consequently, the mean lateral flake sizes obtained from our work were approximately 9, 3, 2 and 1 corresponding to samples A (45 mins), B (90 mins), C (135 mins) and D (180 mins).

However, in order to verify whether or not there was an introduction of basal plane defect into our graphene during the shearing process, a graph of I_D/I_G versus I_D'/I_G was plotted (see figure 6), and a slope of 2.21 obtained. Eckmann et al reported a slope of approximately 3.5 for edge defect, 7.0 for vacancy in the basal plane, and 13 for sp^3 defects [24].

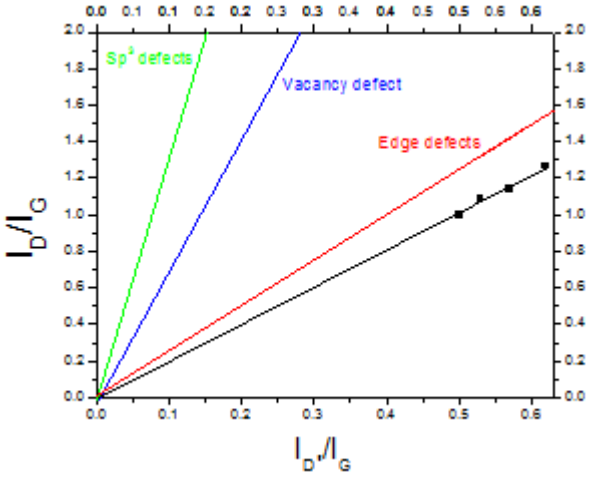

Figure 6: Ratio of intensities of D:G versus D':G for size evaluated graphene prepared through anionic surfactant shear method as compared to Eckmann's et al [24]

This departure from the edge-, vacancy- and sp^3 defect curves proves that no basal plane defect was introduced into our shear exfoliated graphene, under turbulent condition.

4. Conclusions

In this paper, we have reported a facile and replicable route to graphene production using anionic surfactant and hydrotropes contained in household washing liquid. The graphene produced was not tainted with graphene oxide. This was confirmed by EDX measurement which revealed high weight percentage yield (84.49%). Raman characterization showed the exfoliation of graphene monolayer, 2 layer graphene, 3 layer graphene, 9 layer graphene, a D:G intensity band ratio of 0.48 for our starting powder (note that this is different for different source of graphite) and a slope of 2.21, from our I_D/I_G versus I_D'/I_G plot. This is a strong in indication that during the shearing process, no basal or edge defect was introduced in our graphene. Ab-initio calculations [25] simulated graphene of sp^3 type to be approximately 1.3, whereas Eckmann et al experiment put it at 13 [24]. The discrepancy adduced by the experimental group must have introduced so much error that their "hopping" component of the defect must have been exaggerated. We therefore conclude that our 2.21 slope must be somewhere between the cone bounded by edge and sp^3 defects.

5. Acknowledgements

I am grateful to Late Prof. B. N. Onwuagba of the Department of Physics, Federal University of Technology, Owerri, Nigeria, for facilitating the approval of TETFUND grant for characterization my samples.

References

[1] Geim A. K. and Novoselov K. S; The rise of graphene. Nature materials, **6**, 183-1912 (2007)
[2] Mattevi, C., Eda, G., Agnoli, S., Miller, S., Mkhoyan, K. A., Celik, O., Mastrogiovanni, D., Granozzi, G., Garfunkel, E., and Chhowalla, M.; Evolution of electrical, chemical, and structural properties of a transparent and conducting chemically derived graphene thin films. Advanced functional materials, **19**, 2577-2583 (2009).
[3] Lee, C., Wei, X., Kysar, J. W., and Hone, J.; Measurement of the Elastic Properties and Intrinsic Strength of Monolayer Graphene. Science **321**, 385–388 (2008).
[4] Balandin, A. A.; Thermal properties of graphene and nanostructured carbon materials. Nature materials, **10**, 569-581 (2011)
[5] Sun, P., Wang, K., Wei, J., Zhong, M., Wu, D., and Zhu, H.; Magnetic transition in graphene derivatives. Nano Research, DOI 10.1007/s12274-014-0512-1, (2014)
[6] Dresselhaus, M. S., and Dresselhaus, G.; Intercalation compounds of graphite. Adv. Phys. **30**, 139–326 (1981).
[7] Janowska, I, Ersen, O, Jacob, T, Vennégues, P, Bégin, D, Ledoux, M. and Pham-Huu, C; Catalytic unzipping of carbon nanotubes to few-layer graphene sheets under microwaves irradiation. Applied Catalysis A: General **371,** 22-30 (2009).
[8] Chen, G. H. et al. Preparation and characterization of graphite nanosheets from ultrasonic powdering technique. Carbon **42**, 753–759 (2004).
[9] Jung, I. et al. Simple approach for high-contrast optical imaging and characterization of graphene based sheets. Nano Lett. **7**, 3569–3575 (2007).
[10] Wang, S., Zhang, Y., Abidi, N. and Cabrales, L.; Wettability and surface free energy of graphene films. Langmuir 25 (18), 11078-11081 (2009)
[11] Kern, K., David, R, Palmer, R. L,. and Cosma, G.; Complete wetting on 'Strong' substrates Xe/Pt(111) Physical Review letters 56: 2823-2826 (1986)
[12] Pope, S. B.; Turbulent Flows. (Cambridge University Press, 2000).
[13] Utomo, A. T, Baker, M., and Pacek, A. W.; Flow pattern, periodicity and energy dissipation in a batch rotor-stator mixer. Chem. Eng. Res. Des. **86**, 1397-1409, (2008).
[14] Marchisio, D. L, Soos, M, Sefcik, J. and Morbidelli, M; Role of turbulent shear rate distribution in aggregation and breakage processes. AIChE J. **52**, 158-173, (2006).
[15] Boxall, J. A., Koh, C. A., Sloan, E. D., Sum, A. K., and Wu, D. T.; Droplet Size Scaling of Water-in-Oil Emulsions under Turbulent Flow. *Langmuir* **28**, 104-110, (2012).
[16] Ferrari, A. C., and Basko, D. M.; Raman Spectroscopy as a Versatile Tool for Studying the Properties of Graphene. Nature Nanotechnology, 8, 235–246 (2013).
[17] Jorio, A., Dressehlhaus M., Saito, R., Dresselhaus, G. F.; Raman Spectroscopy in Graphene Related Systems; Wiley-VCH, (2011)
[18] Cong, C., Yu, T., Saito, R., Dresselhaus, G. F., Dresselhaus, M. S.; Second-Order Overtone and Combination Raman Modes of Graphene Layers in the Range of 1690-2150 cm^{-1}. ACS Nano, 5, 1600–1605 (2011).
[19] Foa Torres, L. E. F., Roche, S, Charlier, J. C; Introduction to Graphene-Based Nanomaterials: From Electronic Structure to Quantum Transport; Cambridge University Press, 2014.
[20] Castro Neto, A. H., Guinea, F, Peres, N. M. R, Novoselov, K. S., and Geim, A. K.; The electronnic

properties of graphene. Rev. of Mod. Phys., **81, No 1,** (2009).
[21] O'Neill, A., Khan, U., Nirmalraj, P. N., Boland, J., and Coleman, J. N.; Graphene Dispersion and Exfoliation in Low Boiling Point Solvents. Journal of Physical Chemistry C **115**, 5422-5428, (2011).
[22] Khan, U., O'Neill, A., Lotya, M., De, S., and Coleman, J. N.; High-Concentration Solvent Exfoliation of Graphene. Small **6**, 864-871, (2010).
[23] Khan, U. et al.; Size selection of dispersed, exfoliated graphene flakes by controlled centrifugation. Carbon **50**, 470-475, (2012).
[24] Eckmann, A., Felten, A., Mishchenko, A., Britnell, L., Krupke, R.., Novoselov, K. S., Casiraghi, C.; Probing the Nature of Defects in Graphene by Raman Spectroscopy. *Nano Lett.* **12**, 3925-3930, (2012).
[25] Venezuela, P., Lazzeri, M., and Mauri, F. *Phys. Rev. B*, **2011**, *84*, 035433